



Modification of starch-derived graphene quantum dots as multifunctional nanofillers to produce polymer starch/polyvinyl alcohol composite films for active packaging

Qi Sun ^{*}, Lei Zhang, Meiqi Huang, Miaomiao Ma, Jian Zeng, Tao Le ^{**}

College of Life Sciences, Chongqing Normal University, No.37 Chengzhong Road, Shapingba District, Chongqing, 401331, China

ARTICLE INFO

Keywords:

Corn starch
Graphene quantum dots
Nanocomposite film
Active food packaging

ABSTRACT

Here we reported a facile and green route to prepare graphene quantum dots (GQDs) by using corn starch as a nanofiller for the preparation of starch-based active films. The aqueous solution of GQDs displayed excitation wavelength-independent emission, stable photoluminescence, and good bio-safety. And the results demonstrated that the starch-derived GQDs have good compatibility with the natural polymer starch/polyvinyl alcohol (PVA) matrix. With the addition of GQDs over 50 µg/mL, the composite film has a very satisfactory UV blocking capacity. Moreover, 100 µg/mL of GQDs significantly increases the elongation at break and tensile strength of the obtained film to 1.79 and 2.94 times respectively, while the water solubility is only 53.9% of that of the starch/PVA film. The maximum scavenging rates of 2,2-diphenyl-1-picrylhydrazyl free radical by the starch/PVA film containing 150 µg/mL of GQDs was 83.3%. As the amount of GQDs added increases, the inhibitory effect of the composite film on *Staphylococcus aureus* and *Escherichia coli* becomes more and more significant. The starch-sourced composite film's eco-friendly nature and superior performance make it a promising alternative to traditional plastic materials for active packaging.

1. Introduction

The extensive utilization of petroleum-based plastics has resulted in significant environmental pollution. To tackle this problem, there has been a growing demand for sustainable packaging film materials that can be easily decomposed and recycled (Deng et al., 2022; Ezati, Riahi, & Rhim, 2021; Sani & Alizadeh, 2022; Zhang et al., 2022). Starch films are increasingly being considered as viable substitutes for petroleum-based plastics in food packaging. This is primarily attributed to their biodegradability, renewable nature, wide availability, and cost-effectiveness (Fazeli & Lipponen, 2022; Wang et al., 2023). However, the hydrophilicity of starch can have a significant impact on the key functional properties of films, including moisture resistance and mechanical properties (Kumar, Ghoshal, & Goyal, 2019). Moreover, starch films alone do not possess crucial functional properties like antibacterial and UV resistance, which are essential for meeting the current requirements of food packaging. Currently, there is a strong emphasis on the development and enhancement of natural polymer-based films. This involves the integration of various substances,

including natural active agents (Mustafa et al., 2020), biocompatible macromolecular polymers (Khan et al., 2021; Khan & Sadiq, 2021), and nanomaterials (Wang et al., 2022). By incorporating these substances into starch melts, the mechanical, optical, and barrier properties of packaging films can be greatly improved (Pan, Liang, & Gao, 2022; Yang et al., 2021). For example, the incorporation of carvacrol nano-emulsion can greatly enhance the functional characteristics of the resulting starch-based active films (Mao, Li, Zhou, Lu, & Zhang, 2023).

Compared to traditional semiconductor quantum dots, luminescent carbon dots (CDs) show promise for use in active packaging as nanofillers. This is due to their simple preparation, low toxicity, good water solubility, easy functionalization, excellent optical properties, and high compatibility with polymer matrices and other film-forming materials (Shi et al., 2019). Various types of carbon dots, such as carbon quantum dots (CQDs), graphene quantum dots (GQDs), and carbonized polymer dots (CPDs) (Rigodanza et al., 2021), are employed in biological imaging (He et al., 2023), sensing detection (Sun, Zhang, Bhandari, & Yang, 2022), and other domains. Recently, researchers have demonstrated that the oxidized Dialdehyde Persian gum/gelatin film with CDs

^{*} Corresponding author. College of Life Sciences, Chongqing Normal University, Chongqing, 401331, China.

^{**} Corresponding author.

E-mail addresses: sunqi2017@cqnu.edu.cn (Q. Sun), letao@cqnu.edu.cn (T. Le).

exhibits excellent antioxidant and antibacterial activities (Khoshkala-lampour, Ghorbani, & Ghasempour, 2023). The thermal stability and mechanical properties of the isolated mung bean protein-based nanocomposite film are significantly enhanced by the addition of CQDs (Sani & Alizadeh, 2022). Additionally, the inclusion of CD's can give the film unique fluorescent properties (Zhao, Zhang, Mujumdar, Adhikari, & Wang, 2022). These functional properties are crucial for the application of polymeric packaging films (El-Shamy & Zayed, 2020).

Inspired by their excellent properties and potential applications, graphene quantum dots (GQDs) have emerged as a new type of CDs with promising prospects in active packaging. However, the conventional methods used for GQD preparation are known to be cumbersome, hazardous, and contribute to environmental pollution. Developing and investigating suitable GQDs for application as functional and sustainable packaging fillers has become imperative. In this study, we explored the use of the natural polymer starch as a green precursor for GQD synthesis through the hydrothermal method. The novelty of this work lies in examining the functional characteristics of starch/PVA film integrated with starch-sourced GQDs for active packaging. We extensively evaluated the mechanical, optical properties, water resistance, UV barrier, antioxidant, and antibacterial properties of the nanocomposite films prepared. Furthermore, we proposed a potential mechanism for enhancing the performance of starch-based active film by incorporating GQDs.

The prepared nanocomposite films' mechanical, optical properties, water resistance, UV barrier, antioxidant, and antibacterial properties were extensively evaluated. A possible mechanism for enhancing the performance of starch-based active film by incorporating GQDs was further proposed.

2. Materials and methods

2.1. Chemical and reagents

The corn starch used to synthesize graphene quantum dots (GQDs) was bought from Liangrun Whole Grain Food Co., Ltd, Henan province, China. Branched Polyethylenimine (PEI; M.W. 25 kDa), sodium alginate, glycerol, and other analytical grade chemicals were purchased from Aladdin (Shanghai, China) and were not further purified. Deionized water (18 mΩ, Millipore systems) was used throughout the experiment. *Staphylococcus aureus* (ATCC 29213) and *Escherichia coli* (ATCC 43894) were obtained from the Institute of Microbiology, Chinese Academy of Sciences.

2.2. Synthesis of starch-derived GQDs

The corn starch and PEI were firstly dispersed with a 2:1 mass ratio in 25 mL deionized water and stirred at 60 °C for 15 min. The mixed solution was immediately poured into a 50 mL Teflon-lined stainless autoclave, then heated in an oven at 190 °C for 120 min. Then, the autoclave was taken out to be cool freely. The final brown product was transferred to centrifugal tubes, and centrifuged at 10,000 g for 20 min to separate the precipitate. Finished GQD products were obtained by freeze-drying the obtained solution.

2.3. Characterization methods

The morphology and superstructure of the prepared starch-derived GQDs were firstly analyzed with transmission electron microscopy (TEM, JEOL, JEM-2100, Tokyo, Japan), and the accelerating voltage was 200 kV. The fluorescence and UV spectra of as-synthesized GQDs were measured with fluorescence (HITACHI, F-7000, Fukuoka, Japan) and UV-Vis (PerkinElmer, Lambda 35, Waltham, MA, USA) spectrophotometers, respectively. The Fourier transform infrared (FTIR) spectrum of GQDs was collected on a Nicolet-iS10 FTIR instrument (Thermo Scientific, Waltham, MA, USA) equipped with an attenuated total

reflectance (ATR) accessory. The spectrum was performed over a range of (500–4000 cm⁻¹) with 16 scans and a resolution of 8 (0.964 cm⁻¹). Film thickness was recorded using a digital hand-held micrometer (Airaj, Model AI-1127, China) with an accuracy of 0.001 mm. The values obtained from 10 random positions were averaged for the film thickness evaluation for each film sample. The mechanical tensile characteristics of the films were performed using Dynamic mechanical analysis (DMA Q800, TA Instrument, USA). The samples were cut into dumbbell-shaped specimens and measured using a strain amplitude of 0.10% at 1 Hz with a preload force of 0.1 N in oscillatory film tension mode at room temperature in the unaligned direction. Mechanical analysis of each film was calculated using the average thickness of the specimen and at least five specimens per sample were tested. The tensile properties studied were tensile strength (TS) and elongation at break (EAB).

2.4. Production of the polymer starch/polyvinyl alcohol-based composite film

Natural corn starch and polyvinyl alcohol (PVA) were firstly dispersed with a 2:1 mass ratio in 20 mL deionized water and stirred at 75 °C for 40 min. Then, 0.1 g of glycerol and sodium alginate were added to the above-mixed solution and stirred well. Different concentrations of GQD solutions were added to the obtained film-forming solution. The final concentrations of GQDs were 0, 50, 100, and 150 µg/mL. Finally, 20 mL of the prepared film-forming solution was poured into a 10 × 10 cm plastic plate, then dried for 24 h at 25 ± 2 °C to obtain starch/PVA-based films. According to the concentration of GQDs (50, 100, and 150 µg/mL), complex films were labeled as complex + QDs-1, complex + QDs-2, and complex + QDs-3, respectively.

2.5. Cytotoxicity evaluation of starch-sourced GQDs

The cytotoxicity of as-prepared GQDs was evaluated by Thiazolyl blue tetrazolium reduction (MTT) using Ges-1 human gastric mucosal epithelial cells (Sun et al., 2021). First 5.0 × 10³ cells in the logarithmic phase were seeded in 96-well with 100 µL media containing 10% fetal bovine serum and cultured at 37 °C for 24 h. Then, cells were mixed with the different GQD concentrations (100 µL) for 24 h, washed with PBS, and treated with 200 µL of 5 mg/mL MTT in serum-free media. After 4 h, formazan crystals in each well were dissolved in 150 µL of dimethyl sulfoxide. The absorbance of each sample was measured by using a Microplate reader (EPOCH2T, USA) at 570 nm. The viability was calculated as follows:

$$R (\%) = \frac{B}{A} \times 100$$

R (%) = (B/A) × 100, where R represents the cell viability, A is the value of untreated cells, and B is the value of treated cells.

2.6. Film solubility in water

The water solubility of the prepared films was estimated as previously published reported (Ocak, 2018). Film samples were first immersed in distilled water at room temperature for 24 h, and the undissolved portions were filtered out. The undissolved film was weighed after drying in a laboratory oven at 25 °C. The film solubility (%) was calculated as follows:

$$S = \frac{W_b - W_a}{W_b} \times 100$$

where S is the film solubility in water (%); W_b is the initial weight of the film sample (g); W_a is the weight of the dry sample after being immersed.



Scheme 1. Schematic diagram of graphene quantum dots (GQDs) prepared from corn starch by hydrothermal method.

2.7. UV blocking properties

To evaluate the UV-blocking properties, films' absorption and transmission spectra were analyzed by a UV-Vis spectrophotometer (PerkinElmer, Lambda 35, Waltham, MA, USA) (Patil et al., 2020). Film samples were cut into 10 mm × 40 mm strips and placed in a quartz cuvette for full wavelength scanning from 200 to 800 nm.

2.8. Antioxidant capacities

The 2,2-diphenyl-1-picrylhydrazyl (DPPH) scavenging test was carried out as previously described with modifications (Jamróz et al., 2019). A newly prepared ethanolic DPPH solution (4 mL, 0.1 mM) was mixed with 0.1 g of film samples with different GQD concentrations. After reacting for 30 min in the dark, the absorbances of the DPPH solution (A_0) and DPPH solution with film sample (A_i) at 517 nm were recorded. The DPPH scavenging rate of films was calculated as follows: DPPH scavenging capacity (%) = $(1 - A_i/A_0) \times 100\%$.

2.9. Antibacterial activity

The antibacterial activity of film-forming solutions was investigated using agar diffusion (Kousheh, Moradi, Tajik, & Molaei, 2020). *S. aureus*

and *E. coli* were the test bacterial strains. Starch/PVA solutions with different GQD concentrations (0, 50, 100, and 150 µg/mL) were loaded onto sterilized filtering papers (5 mm diameter). The bacterial strains (about 10^4 – 10^5 CFU/mL) uniformly covered the surface of the nutrient broth agar plates, and the filtering papers were laid on the agar surface. The plates were incubated at 37 °C overnight, and the diameter of the inhibition zones was measured.

2.10. Statistical analysis

All experiments were performed at least in triplicates, and the data are expressed as means ± standard deviations. Significant differences were determined using Duncan's multiple test ($p < 0.05$) after a one-way analysis of variance (ANOVA). Statistical analyses were conducted using SPSS version 22.0 (SPSS Inc., USA).

3. Results and discussion

3.1. Synthesis mechanism and characterizations of starch-derived GQDs

In this study, a green and facile one-pot hydrothermal method was used to synthesize GQDs using natural polymeric starch as a new precursor (Scheme 1). The synthesis mechanism of GQDs prepared from

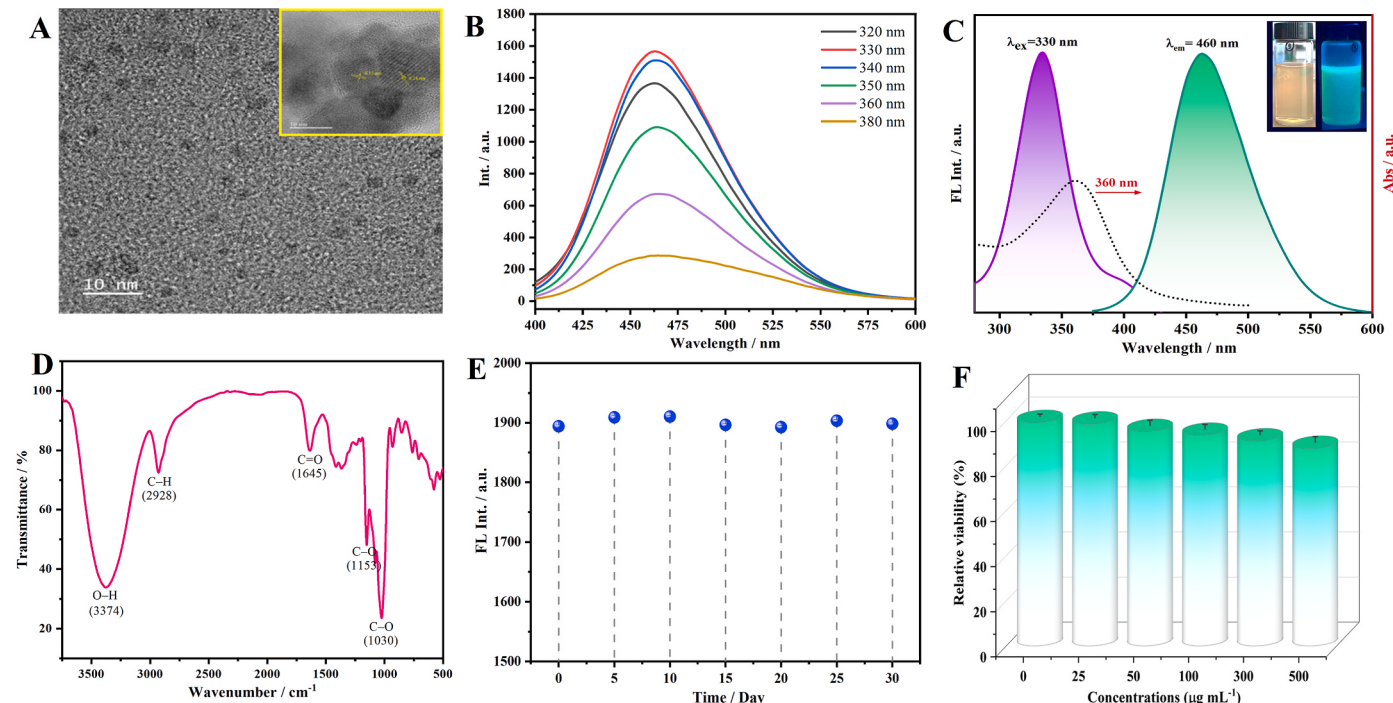


Fig. 1. (A) High-resolution transmission electron micrograph observation, (B) fluorescence spectra at different excitation wavelengths, (C) UV-Vis absorption and fluorescence excitation and emission spectra, (D) Fourier transmission infrared spectroscopy, and (E) Fluorescence stability and (F) cytotoxicity evaluation of as-synthesized starch-derived graphene quantum dots (GQDs).

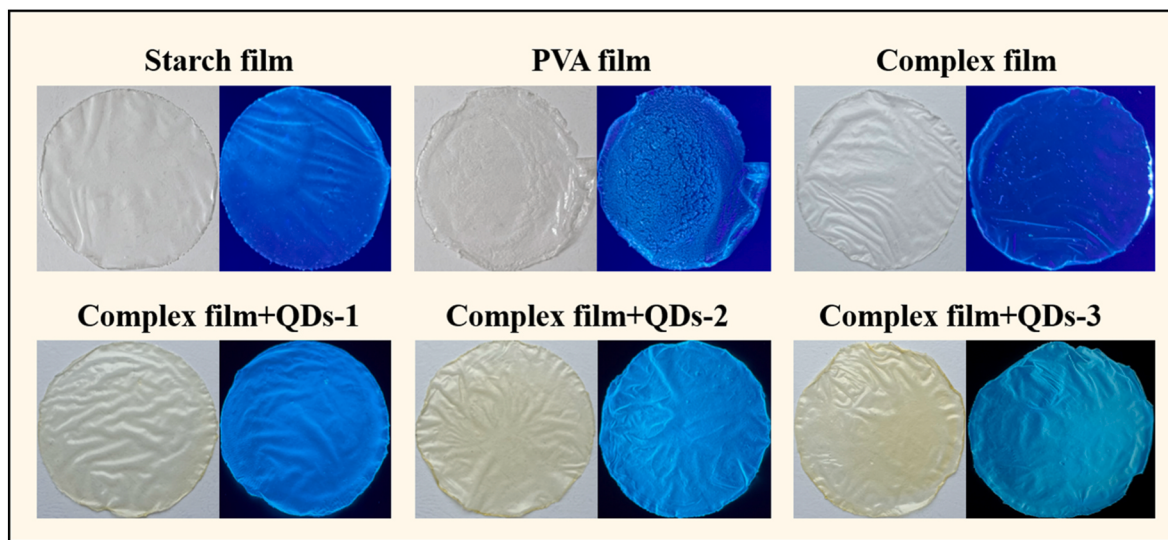


Fig. 2. Images of the obtained film samples under sunlight and UV light (365 nm) irradiation.

corn starch consists mainly of starch hydrolysis and subsequent ring-closure condensation reactions. Under hydrothermal conditions, starch can be converted in a small batch reactor through hydrolysis with water mainly to glucose and other relatively low-level carbohydrates without the addition of any additives (Nagamori & Funazukuri, 2004). Next, the hydrogen atom of the glucose molecule interacts with the hydroxyl group of the adjacent glucose molecule, and the formyl group reacts with the hydroxyl group, leading to dehydration under hydrothermal conditions (Bayat & Saievar-Iranizad, 2017). As a result, carbon atoms covalently interact with each other and finally GQDs are formed. On the other hand, other residual carbon hydrates are transformed into carbide precipitates due to carbonization at high temperature and pressure.

The morphology of the prepared GQDs was approximately almost spherical with a uniform distribution of 8.41 nm (Fig. 1A). The high-resolution transmission electron microscopy (HRTEM) indicated a measured lattice spacing of 0.24 nm and 0.35 nm (Fig. 1A), which is in good agreement with (020) and (002) planes of graphitic carbon (JCPDS 26–1076), respectively (Chen et al., 2018). Next, photo-luminescence spectroscopy was conducted to evaluate the intrinsic luminescence characteristics of starch-sourced GQDs. The as-synthesized GQDs displayed excitation-independent emission features (Fig. 1B). Therefore, the prepared starch-sourced GQDs exhibited independent excitation wavelengths. The optimal excitation and emission wavelengths were 330 and 460 nm, respectively (Fig. 1C). The aqueous dispersion of GQDs appeared pale-yellow under sunlight illumination and turned brilliant green under 365 nm irradiation (inset of Fig. 1C). The UV–Vis spectra of GQDs showed a maximum absorption peak at 360 nm (Fig. 1C), demonstrating that the n–π* transition of the C=O bond. The Fourier

transforms infrared (FT-IR) spectra (Fig. 1D) show a broad peak at 3374 cm⁻¹ corresponding to the stretching vibration of O–H and another peak at 2928 cm⁻¹ corresponding to the stretching vibration of C–H. Additionally, there are peaks at 1645 cm⁻¹ and 1421 cm⁻¹, which align with the skeletal vibration of aromatic rings of GQDs, indicating the honeycomb lattice structure of graphene. Furthermore, the peaks observed in the range of 500–1100 cm⁻¹ can be attributed to the C–O stretching vibration. Meanwhile, the prepared GQDs had good fluorescent stability and exhibited a decrease in the fluorescence intensity to a maximum of 5.1% (Fig. 1E). Moreover, the MTT test was applied to evaluate the cytotoxicity of GQDs, the cell viability remained over 85% when the concentration of GQDs increased from 25 to 500 µg/mL (Fig. 1F). Nevertheless, the maximum concentration of GQDs used in this study was only 150 µg/mL. Overall, the prepared starch-derived GQDs had low cytotoxicity and excellent biocompatibility, which are suitable for the potential film application.

3.2. Optical properties

Corn starch presented good film-forming properties, but PVA did not (Fig. 2). Combining the two (denoted as complex film) significantly improved the overall performance of the as-prepared film. Pure starch and PVA or complex films had no fluorescence signal under UV light irradiation (320–380 nm). However, the complex films containing 50, 100, and 150 µg/mL of GQDs displayed bright blue fluorescence under UV light irradiation, consistent with the fluorescence characteristics of as-synthesized GQDs. Besides, the fluorescence intensity did not significantly increase with increasing the concentrations of GQD, possibly due

Table 1
Physical and functional characteristics of different film samples.

Sample	GQDs additions (µg/mL)	Thickness (µm)	Tensile strength (MPa)	Elongation at break (%)	Water solubility (%)	Free radical scavenging rate (%)
Starch film	0	51.23 ± 1.27 ^a	1.81 ± 0.09 ^b	136.81 ± 6.84 ^a	60.81 ± 3.04 ^b	2.98 ± 0.15 ^e
PVA film	0	50.83 ± 2.11 ^a	0.80 ± 0.04 ^d	89.37 ± 4.47 ^b	91.62 ± 4.58 ^a	6.08 ± 0.31 ^d
Complex film	0	53.54 ± 2.67 ^a	1.46 ± 0.07 ^c	51.50 ± 2.57 ^d	50.84 ± 2.54 ^c	5.66 ± 0.28 ^d
Complex film + QDs-1	50	55.19 ± 3.01 ^a	1.76 ± 0.09 ^b	78.37 ± 3.92 ^c	46.32 ± 2.32 ^d	18.13 ± 0.91 ^c
Complex film + QDs-2	100	54.82 ± 2.39 ^a	2.35 ± 0.11 ^a	92.20 ± 4.61 ^b	27.44 ± 1.37 ^e	43.88 ± 2.19 ^a
Complex film + QDs-3	150	55.78 ± 1.73 ^a	1.77 ± 0.09 ^b	82.63 ± 4.13 ^c	42.81 ± 2.14 ^d	36.55 ± 1.83 ^b

* Complex film represents Starch/PVA film.

** Data are the means ± standard deviations and different superscript letters in the same column indicates significant differences ($p < 0.05$).

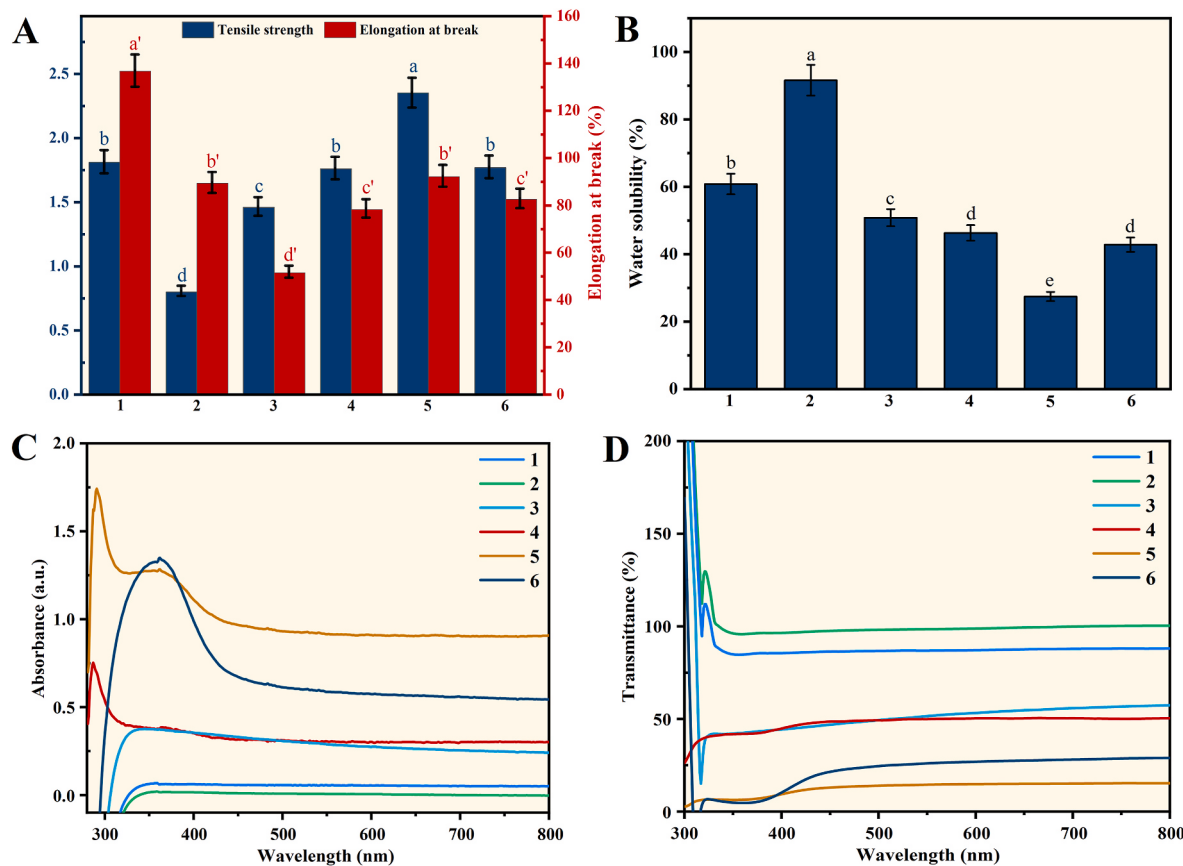


Fig. 3. (A) Mechanical properties, (B) water solubility, (C) UV-vis absorption spectra, and (D) transmittance spectrum of the resulting films. 1-Starch film, 2-PVA film, 3-Complex film, 4-Complex film+50 µg/mL of GQDs, 5-Complex film+100 µg/mL of GQDs, and 6-Complex film+150 µg/mL of GQDs. Graph bars with different letters on top represent statistically significant results ($p < 0.05$) based on one-way analysis of variance (ANOVA).

to the increase in film thickness and the decrease in light transmittance. Additionally, the opacity of the obtained film significantly increased as the GQD addition in the solution increased (Fig. 2). Generally, packaging materials with low transparency are preferred for packaging food.

3.3. Mechanical properties and water solubility

As expected, the thickness of as-prepared films gradually increased from 51.23 to 55.78 µm after incorporating different GQD concentrations (Table 1). However, the thickness of the starch/PVA complex film containing GQDs did not differ from pure starch, PVA, or complex films without GQDs ($p > 0.05$). This result might be related to the small particle size of GQDs and the low concentration used. On the other hand, tensile strength (TS) and elongation at break (EAB) are commonly related to the magnitude of intermolecular force and microstructure, indicating the toughness and strength of the obtained films, respectively. The introduction of GQDs significantly improved the mechanical properties of the starch/PVA-based film (Fig. 3A). The TS value of complex + QD-2 film with 100 µg/mL of GQDs was significantly higher ($p < 0.05$) than other films (Table 1). Meanwhile, the decreased EAB value was obtained for starch/PVA complex film without GQDs, resulting in remarkably weakened flexibility. However, this unfavorable phenomenon was significantly improved with GQD addition, especially when the GQD concentration was 100 µg/mL (Fig. 3A). Therefore, the overall mechanical performance of the starch/PVA-based film was enhanced, due to the strong hydrogen bonds on the GQD surface and -OH/-COOH in PVA chains (Rani, Kumar, Mandal, & Kumar, 2020).

The water resistance and integrity of packaging films, which can be determined by water solubility, are crucial for food preservation. Starch and PVA films are known for their low water resistance due to their

hydrophilic nature. As shown in Table 1, significant differences ($p < 0.05$) were found for the water solubility of both films (60.81% for starch film and 91.62% for PVA film). Meanwhile, the water solubility ranged from 46.32 to 27.44% for complex films containing GQD concentrations between 0 and 150 µg/mL. However, a film solubility decreasing trend was not observed with increasing the level of GQDs. Different composite films also significantly differed ($p < 0.05$), and the complex film with 100 µg/mL of GQDs exhibited the lowest solubility. Thus, GQD addition significantly decreased film water solubility compared to the control films, which might be explained by the cross-linking of GQDs and the hydrophilic groups on the starch or PVA chain, weakening the interaction between hydrophilic groups and surrounding molecules (Rahman, Mujeeb, & Muraleedharan, 2017).

3.4. UV blocking properties

The ability of the films to block UV irradiation is an important attribute for food packaging (Nguyen & Lee, 2022). Thus, the UV-Vis absorption spectra measurement was applied to evaluate the UV barrier capacities of different films. Pure starch or PVA films displayed almost no UV absorption peak and had a very small absorption peak in the 300–800 nm wavelength. GQD addition significantly increased the absorption value of starch/PVA complex films in 300–800 nm wavelengths. Since GQDs had strong UV absorption at 270 and 360 nm, a clear absorption peak appeared in the complex + QD-2 film with 100 µg/mL of GQDs (Fig. 3C). The UV-Vis scanning was performed in the transmittance mode to understand the efficiency of GQDs on the UV shielding properties of the composite films. The PVA film presented the maximum UV transmittance capacity, followed by the starch film. The UV transmittance of the starch/PVA composite film significantly

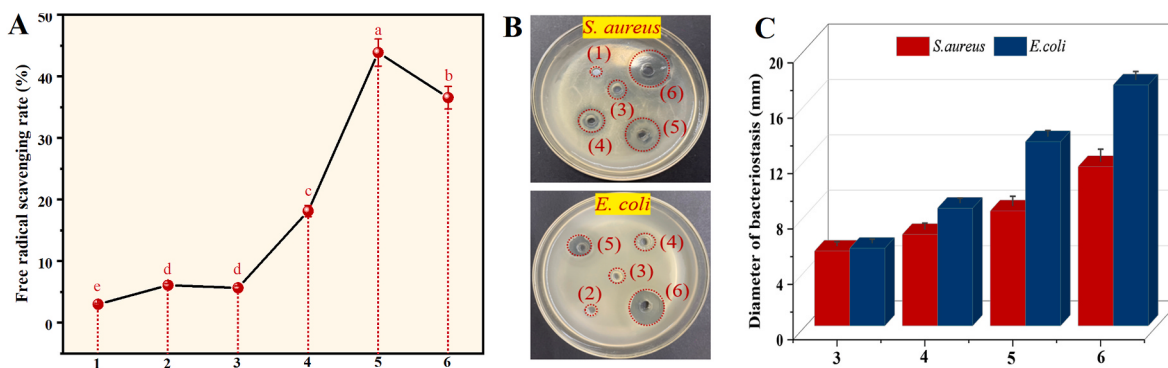


Fig. 4. (A) Antioxidant activities, (B) pictures of the inhibition zone against *S. aureus* and *E. coli*, and (C) antibacterial efficiency of the prepared films. 1-Starch film, 2-PVA film, 3-Complex film, 4-Complex film+50 µg/mL of GQDs, 5-Complex film+100 µg/mL of GQDs, and 6-Complex film+150 µg/mL of GQDs. Graph bars with different letters on top represent statistically significant results ($p < 0.05$) based on one-way analysis of variance (ANOVA).

decreased in the 300–800 nm range with increasing GQD concentrations. When the GQD concentrations was over 50 µg/mL, the obtained films could completely block the light at 300–400 nm wavelength. These results indicated that the best UV-blocking performance was achieved when GQDs were added at more than 50 µg/mL.

3.5. Antioxidant and antibacterial activities

It is well-known that CDs have excellent antioxidant activities due to the existence of many electron donor groups on their surface, including hydroxyl and carboxyl groups. The pure starch film had almost no scavenging effect on DPPH free radicals (Fig. 4A). The scavenging rate of DPPH radicals by pure PVA and starch/PVA complex films without GQDs was below 6.1%. However, when the GQD concentration was 50 µg/mL, the DPPH clearance significantly increased to 18.2%. The starch/PVA-based composite film achieved DPPH radical scavenging rate (43.9%) when the GQD concentrations was 100 µg/mL. The complex film with the highest GQD level (150 µg/mL) could reach the 83.3% of DPPH scavenging rate (Table 1). Therefore, the strong free radical scavenging capacity of GQDs endows the starch/PVA composite film with good antioxidant activity.

The antibacterial performance of starch/PVA-based film against two common bacteria (*S. aureus* and *E. coli*) was evaluated using the agar disc diffusion method (Fig. 4B). Pure starch/PVA mixed solution without GQDs displayed no antibacterial activity, and GQD addition imparted antibacterial properties to the film-formed solution. The quantum size effect of GQDs endows it with more oxygen-containing functional groups and causes it to increase the oxidative stress effect for killing bacteria (Kousheh et al., 2020). With GQD concentrations from 50 to 150 µg/mL, the inhibition zone diameters of starch/PVA mixed solution against *S. aureus* and *E. coli* significantly increased from 8.5 to 6.6 mm to 17.4 and 11.5 mm (Fig. 4C), respectively ($p < 0.05$); the antibacterial effect of the film-forming solution was more significant with GQD concentration of 250 µg/mL. The different inhibitory effects on bacteria are mainly due to differences in their composition and cell wall structures (Varghese & Balachandran, 2021).

4. Conclusions

The present study aimed to identify a facile, sustainable, and effective method for synthesizing graphene quantum dots (GQDs) using corn starch as a new precursor. The GQDs derived from starch, when modified with polyethyleneimine, exhibited a uniformly dispersed spherical structure and excitation-independent emission features. Additionally, the synthesized GQDs demonstrated good hydrophilicity, high biosafety, and strong fluorescence emission. The study also successfully prepared corn starch-based composite films, following green and sustainable development practices. By incorporating multifunctional GQDs into the

starch/polyvinyl alcohol (PVA) matrix, the resulting films exhibited improved opacity, enhanced mechanical properties, water resistance capacity, and UV-blocking properties. Moreover, the addition of GQDs endowed the starch/PVA-based film with antioxidant properties and antibacterial activities. The composite film showed the best overall performance when the GQD concentration was 100 µg/mL. Thus, this research highlights a green and sustainable strategy for utilizing starch-derived functional nanofillers and starch-based natural films in active packaging applications.

CRediT authorship contribution statement

Qi Sun: Writing – review & editing, Writing – original draft, Visualization, Methodology, Data curation, Conceptualization. **Lei Zhang:** Software, Methodology, Investigation, Data curation. **Meiqi Huang:** Visualization, Software. **Miaomiao Ma:** Software, Data curation. **Jian Zeng:** Validation. **Tao Le:** Supervision, Project administration, Funding acquisition.

Declaration of competing interest

The authors declare that they have no known competing financial interests or personal relationships that could have appeared to influence the work reported in this paper.

Data availability

The authors do not have permission to share data.

Acknowledgements

The work was financially supported by grants from the Science and Technology Research Program of Chongqing Municipal Education Commission (KJQN202100516).

References

- Bayat, A., & Saievar-Iranizad, E. (2017). Synthesis of green-photoluminescent single layer graphene quantum dots: Determination of HOMO and LUMO energy states. *Journal of Luminescence*, 192, 180–183. <https://doi.org/10.1016/j.jlumin.2017.06.055>
- Chen, W., Li, D., Tian, L., Xiang, W., Wang, T., Hu, W., et al. (2018). Synthesis of graphene quantum dots from natural polymer starch for cell imaging. *Green Chemistry*, 20(19), 4438–4442. <https://doi.org/10.1039/C8GC02106F>
- Deng, J., Zhu, E. Q., Xu, G. F., Naik, N., Murugadoss, V., Ma, M. G., et al. (2022). Overview of renewable polysaccharide-based composites for biodegradable food packaging applications. *Green Chemistry*, 24(2), 480–492. <https://doi.org/10.1039/DIGC03898B>
- El-Shamy, A. G., & Zayed, H. S. S. (2020). New polyvinyl alcohol/carbon quantum dots (PVA/CQDs) nanocomposite films: Structural, optical and catalysis properties.

- Synthetic Metals*, 259, Article 116218. <https://doi.org/10.1016/j.synthmet.2019.116218>
- Ezati, P., Riahi, Z., & Rhim, J.-W. (2021). Carrageenan-based functional films integrated with CuO-doped titanium nanotubes for active food-packaging applications. *ACS Sustainable Chemistry & Engineering*, 9(28), 9300–9307. <https://doi.org/10.1021/acssuschemeng.1c01957>
- Fazeli, M., & Lippinen, J. (2022). Developing self-Assembled starch nanoparticles in starch nanocomposite films. *ACS Omega*, 7(49), 44962–44971. <https://doi.org/10.1021/acsomega.2c05251>
- He, Y. F., Cheng, K., Zhong, Z. T., Hou, X. L., An, C. Z., Zhang, J., et al. (2023). Carbon quantum dot fluorescent probe for labeling and imaging of stellate cell on liver frozen section below freezing point. *Analytica Chimica Acta*, 1260, Article 341210. <https://doi.org/10.1016/j.jaca.2023.341210>
- Jamróz, E., Kopel, P., Tkaczewska, J., Dordevic, D., Jancikova, S., Kulawik, P., et al. (2019). Nanocomposite furcellaran films-the influence of nanofillers on functional properties of furcellaran films and effect on linseed oil preservation. *Polymers*, 11 (12), 2046. <https://doi.org/10.3390/polym11122046>
- Khan, N. A., Niazi, M. B. K., Sher, F., Jahan, Z., Noor, T., Azhar, O., et al. (2021). Metal organic frameworks derived sustainable polyvinyl alcohol/starch nanocomposite films as robust materials for packaging applications. *Polymers*, 13(14). <https://doi.org/10.3390/polym13142307>
- Khan, M. R., & Sadiq, M. B. (2021). Importance of gelatin, nanoparticles and their interactions in the formulation of biodegradable composite films: A review. *Polymer Bulletin*, 78(7), 4047–4073. <https://doi.org/10.1007/s00289-020-03283-4>
- Khoshkalamour, A., Ghorbani, M., & Ghasempour, Z. (2023). Cross-linked gelatin film enriched with green carbon quantum dots for bioactive food packaging. *Food Chemistry*, 404, Article 134742. <https://doi.org/10.1016/j.foodchem.2022.134742>
- Kousheh, S. A., Moradi, M., Tajik, H., & Molaei, R. (2020). Preparation of antimicrobial/ultraviolet protective bacterial nanocellulose film with carbon dots synthesized from lactic acid bacteria. *International Journal of Biological Macromolecules*, 155, 216–225. <https://doi.org/10.1016/j.ijbiomac.2020.03.230>
- Kumar, R., Ghoshal, G., & Goyal, M. (2019). Moth bean starch (*Vigna aconitifolia*): Isolation, characterization, and development of edible/biodegradable films. *Journal of Food Science and Technology*, 56(11), 4891–4900. <https://doi.org/10.1007/s13197-019-03959-4>
- Mao, S., Li, F., Zhou, X., Lu, C., & Zhang, T. (2023). Characterization and sustained release study of starch-based films loaded with carvacrol: A promising UV-shielding and bioactive nanocomposite film. *LWT-Food Science and Technology*, 180, Article 114719. <https://doi.org/10.1016/j.lwt.2023.114719>
- Mustafa, P., Niazi, M. B. K., Jahan, Z., Samin, G., Hussain, A., Ahmed, T., et al. (2020). PVA/starch/propolis/anthocyanins rosemary extract composite films as active and intelligent food packaging materials. *Journal of Food Safety*, 40(1). <https://doi.org/10.1111/jfs.12725>
- Nagamori, M., & Funazukuri, T. (2004). Glucose production by hydrolysis of starch under hydrothermal conditions (Vol. 79, pp. 229–233). <https://doi.org/10.1002/jctb.976>, 3.
- Nguyen, S. V., & Lee, B. K. (2022). PVA/CNC/TiO₂ nanocomposite for food-packaging: Improved mechanical, UV/water vapor barrier, and antimicrobial properties. *Carbohydrate Polymers*, 298, Article 120064. <https://doi.org/10.1016/j.carbpol.2022.120064>
- Ocak, B. (2018). Film-forming ability of collagen hydrolysate extracted from leather solid wastes with chitosan. *Environmental Science and Pollution Research*, 25(5), 4643–4655. <https://doi.org/10.1007/s11356-017-0843-z>
- Pan, W., Liang, Q., & Gao, Q. (2022). Preparation of hydroxypropyl starch/polyvinyl alcohol composite nanofibers films and improvement of hydrophobic properties. *International Journal of Biological Macromolecules*, 223, 1297–1307. <https://doi.org/10.1016/j.ijbiomac.2022.11.114>
- Patil, A. S., Waghmare, R. D., Pawar, S. P., Salunkhe, S. T., Kolekar, G. B., Sohn, D., et al. (2020). Photophysical insights of highly transparent, flexible and re-emissive PVA @ WTR-CDs composite thin films: A next generation food packaging material for UV blocking applications. *Journal of Photochemistry and Photobiology A: Chemistry*, 400, Article 112647. <https://doi.org/10.1016/j.jphotochem.2020.112647>
- Rahman, P. M., Mujeeb, V. M. A., & Muraleedharan, K. (2017). Flexible chitosan-nano ZnO antimicrobial pouches as a new material for extending the shelf life of raw meat. *International Journal of Biological Macromolecules*, 97, 382–391. <https://doi.org/10.1016/j.ijbiomac.2017.01.052>
- Rani, S., Kumar, K. D., Mandal, S., & Kumar, R. (2020). Functionalized carbon dot nanoparticles reinforced soy protein isolate biopolymeric film. *Journal of Polymer Research*, 27(10), 312. <https://doi.org/10.1007/s10965-020-02276-1>
- Rigodanza, F., Burian, M., Arcudi, F., Dordević, L., Amenitsch, H., & Prato, M. (2021). Snapshots into carbon dots formation through a combined spectroscopic approach. *Nature Communications*, 12(1), 2640. <https://doi.org/10.1038/s41467-021-22902-w>
- Sani, I. K., & Alizadeh, M. (2022). Isolated mung bean protein-pectin nanocomposite film containing true cardamom extract microencapsulation/CeO₂ nanoparticles/graphite carbon quantum dots: Investigating fluorescence, photocatalytic and antimicrobial properties. *Food Packaging and Shelf Life*, 33, Article 100912. <https://doi.org/10.1016/j.fpsl.2022.100912>
- Shi, X., Wei, W., Fu, Z., Gao, W., Zhang, C., Zhao, Q., et al. (2019). Review on carbon dots in food safety applications. *Talanta*, 194, 809–821. <https://doi.org/10.1016/j.talanta.2018.11.005>
- Sun, D., Mao, J., Cheng, L., Yang, X. L., Li, H., Zhang, L. X., et al. (2021). Magnetic g-C₃N₄/NiFe₂O₄ composite with enhanced activity on photocatalytic disinfection of *Aspergillus flavus*. *Chemical Engineering Journal*, 418, 11. <https://doi.org/10.1016/j.cej.2021.129417>
- Sun, Y., Zhang, M., Bhandari, B., & Yang, C. (2022). Recent development of carbon quantum dots: Biological toxicity, antibacterial properties and application in foods. *Food Reviews International*, 38(7), 1513–1532. <https://doi.org/10.1080/87559129.2020.1818255>
- Varghese, M., & Balachandran, M. (2021). Antibacterial efficiency of carbon dots against gram-positive and gram-negative bacteria: A review. *Journal of Environmental Chemical Engineering*, 9(6), Article 106821. <https://doi.org/10.1016/j.jece.2021.106821>
- Wang, Y., Wang, X., Hu, G., Al-Romaima, A., Liu, X., Bai, X., et al. (2022). Effect of green coffee oil as a natural active emulsifying agent on the properties of corn starch-based films. *LWT-Food Science and Technology*, 170, Article 114087. <https://doi.org/10.1016/j.lwt.2022.114087>
- Wang, W., Zhang, W., Li, L., Deng, W., Liu, M., & Hu, J. (2023). Biodegradable starch-based packaging films incorporated with polyurethane-encapsulated essential-oil microcapsules for sustained food preservation. *International Journal of Biological Macromolecules*, 235, Article 123889. <https://doi.org/10.1016/j.ijbiomac.2023.123889>
- Yang, G., Xia, Y., Lin, Z., Zhang, K., Fatehi, P., & Chen, J. (2021). Physicochemical impact of cellulose nanocrystal on oxidation of starch and starch based composite films. *International Journal of Biological Macromolecules*, 184, 42–49. <https://doi.org/10.1016/j.ijbiomac.2021.06.009>
- Zhang, Y., Jiang, F., Zhao, W., Fu, L., Xu, C., & Lin, B. (2022). One-pot synthesis of degradable and renewable cellulose-based packaging films. *ACS Sustainable Chemistry & Engineering*, 10(50), 16871–16881. <https://doi.org/10.1021/acscuschemeng.2c05440>
- Zhao, L., Zhang, M., Mujumdar, A. S., Adhikari, B., & Wang, H. (2022). Preparation of a novel carbon dot/polyvinyl alcohol composite film and its application in food preservation. *ACS Applied Materials & Interfaces*, 14(33), 37528–37539. <https://doi.org/10.1021/acsami.2c10869>